1 # Effective Locking ~~for Various Phosphorus Pollutants in Water Bodies:~~ of Organophosphate by Lanthanum/Aluminum-Hydroxide Composite

Commented [PG1]:

3 Rui Xu[†,‡], Meiyi Zhang[*,†], and Gang Pan[*,†,‡,§]

4 [†] Research Center for Eco-Environmental Sciences, Chinese Academy of Sciences,

5 Beijing 100085, China

6 [‡] University of Chinese Academy of Sciences, Beijing 100049, China

7 [§] School of Animal, Rural and Environmental Sciences, Nottingham Trent University,

8 Brackenhurst Campus, Nottinghamshire NG25 0QF, United Kingdom

9 * Corresponding author: myzhang@rcees.ac.cn, gpan@rcees.ac.cn

10

ABSTRCT: Lanthanum-bearing materials have been widely used to remove phosphorus (P) especially orthophosphate in water treatment. However, its binding ability and interaction mechanism to other P species in natural waters such as organic phosphate and condensed phosphate are not well understood. Here, a lanthanum/aluminum-hydroxide (LAH) composite was used to investigate its adsorption efficiencies and mechanisms to myo-inositol hexakisphosphate (IHP) and pyrophosphate (Pyro-P) with the contrast of orthophosphate (Ortho-P). The maximum IHP and Pyro-P adsorption capacities by LAH were 36.4 mg P g^{-1} and 21.8 mg P g^{-1}, respectively. Zeta potential, ^{31}P solid-state nuclear magnetic resonance (NMR) spectroscopy and P K-edge X-ray absorption near edge structure (XANES) analyses possibly indicated that the interaction between LAH and P species was surface adsorption by the formation of inner-sphere complexes. Liner combination fitting results of XANES showed that IHP and Pyro-P were preferentially bonded with La-hydroxide in LAH under alkaline conditions (pH 8.5). This work elucidates the adsorption properties and mechanisms of IHP and Pyro-P on lanthanum bearing compounds at the molecular level, indicating that LAH was a promising material for eutrophication control.

Keywords: phosphorus, adsorption, XANES, mechanism, eutrophication control

TOC

30
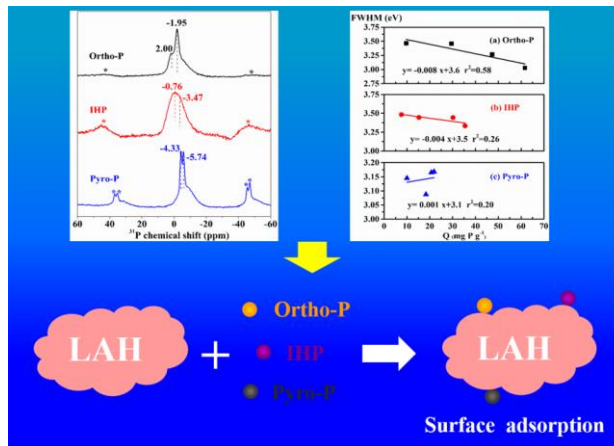
1. INTRODUCTION

Phosphorus (P) is an essential nutrient for biological organisms, but excessive P input is a main factor to trigger eutrophication in freshwater and coastal ecosystem.[1, 2] Over recent decades, great efforts have been made in developing ecologically benign and cost-effective P removal materials.[3] In particular, lanthanum (La) bearing materials have been considered as a useful tool to control P enrichment in lake restoration, owing to its superior P adsorption capacity, low P release rate, and wide applied pH range.[4-7] Previous studies of P removal using La-bearing materials primarily focused on locking inorganic phosphate i.e. orthophosphate (Ortho-P), which is one of the most predominant P species in aquatic ecosystem and can be used by bacteria, algae, and aquatic plants directly.[8-10]

In addition to bioavailable Ortho-P, there are several other species of dissolved P existed in water bodies, such as organic phosphate and condensed phosphate (pyro-, meta-, and polyphosphate).[11] Myo-inositol hexakisphosphate (IHP) is the most abuntant organic phosphate in lake sediments.[12, 13] It can be released into waters under anaerobic conditions and can be used by aquatic organims indirectly.[14] Condensed phosphate for example sodium pyrophosphate (Pyro-P) is widely applied as fertilizers

3

48 in soils and may enter waters through leaching and surface runoff.[15] Furthemore,

49 organic phosphate and condensed phosphate can be hydrolyzed to Ortho-P by

50 extracellular phosphatase or phytases and then may be used as potentially bioavailable

51 P pool for aquatic organisms.[11, 16, 17] Such accumulation of various P species may

52 finally increase the environmental risk of eutrophication.[18] Hence, it is necessary to

53 focus on different P species except for Ortho-P to mitigate eutrophication in

54 geo-engineering for lake restoration.

55 The binding properties of P species on the adsorption materials possibly dominate

56 their behaviors in water bodies. It has been reported that organic phosphate and

57 condensed phosphate are adsorbed on Fe- (hydro)oxide, Al- (hydro)oxide, and

58 titanium dioxide by forming inner-sphere complexes.[19-21] However, little information

59 is available about the fate of organic phosphate and condensed phosphate after

60 La-bearing materials application in aquatic environments. Such lacking of P binding

61 properties with lake restoration materials is not beneficial to understand the potential

62 influence of La-bearing materials and P migration process in water bodies.

63 Solid state nuclear magnetic resonance (SSNMR) spectroscopy is a versatile

64 technique to study the binding mode of different P species on environmental materials,

65 for instance P bonded on iron oxyhydroxides,[22] gibbsite and kaolinite,[23] and

66 amorphous aluminum hydroxide.[24] X-ray absorption near edge structure (XANES)

67 spectroscopy can provide detail information on local chemical environment of the

68 specific element, which has been widely used to distinguish various P species in soils

69 and sediments.[25, 26] By using the element-specific and in situ techniques of ^{31}P

70 SSNMR and P K-edge XANES, we can obtain the molecular level information of

71 different P species associated with La-bearing materials and predict their performance

72 when application in aquatic environments

4

73   Our recent study has demonstrated that lanthanum/aluminum hydroxide composite

74   (LAH) exhibited highly effective adsorption capacity of Ortho-P.[10] These observations

75   promote the hypothesis that LAH may also show an affinity to IHP and Pyro-P existed

76   in water bodies. The objective of this study is to investigate the removal properties of

77   LAH to IHP and Pyro-P and illustrate their adsorption mechanisms at the molecular

78   level. The properties of three P compounds associated with LAH, including potassium

79   dihydrogen phosphate, inositol hexakisphosphate acid sodium salt, and sodium

80   pyrophosphate, were studied by batch experiments and multiple characterization

81   techniques. The experiments of adsorption isotherm, desorption behavior, and

82   adsorption kinetics were conducted to determine the macroscopic binding properties

83   of three P species on LAH. ^{31}P SSNMR and P K-edge XANES techniques were used

84   to explore the microstructures of P bonded on LAH. Liner combination fitting (LCF)

85   analysis was used to investigate the P distribution proportions with La-hydroxide and

86   Al-hydroxide in LAH. The results of our study has demonstrated the interaction

87   mechanism of IHP and Pyro-P with LAH, which is important to design and implement

88   La-bearing materials for eutrophication control.

89   **2. MATERIALS AND METHODS**

90   **2.1. Materials.**

91   Three species of P were used in this study, including potassium dihydrogen

92   phosphate (KH_2PO_4, Ortho-P), inositol hexakisphosphate acid sodium salt

93   ($C_6H_9Na_9O_{24}P_6$, IHP), and sodium pyrophosphate ($Na_4P_2O_7 \cdot 10H_2O$, Pyro-P). All

94   reagents were obtained from sigma-aldrich (Saint Louis, MO, USA). The commercial

95   product Phoslock was purchased from Phoslock Water Solutions Ltd., Australia.

96   **2.2. Preparation of LAH.**

97   LAH was synthesized using the same method described in our previous study.[10]

98   Amounts of analytical grade $LaCl_3 \cdot 7H_2O$ and $AlCl_3$ were dissolved in 200 mL

99   deionized water to obtain a La/Al molar ratio of 1:10 and followed by adding 2 mol

100   L^{-1} NaOH solution at 60 °C until pH 9.0. Then the mixture was stirred at 60 °C for

101   another 2 h. Precipitates were aged for 24 h, then separated by centrifugation, washed

102   with deionized water, and freeze-dried for 24 h. The La mass proportion of LAH was

103   13.1%.[10] Powders of $La(OH)_3$ and $Al(OH)_3$ were synthesized by the same process to

104   act as controls.[10] The detailed characterizations of LAH were published in our

105   previous studies.[10]

106   **2.3. Adsorption and desorption experiments.**

107   The P adsorption experiments were conducted in 50 mL polypropylene tubes at

108   25 °C. LAH (1 g L^{-1}) was mixed with various concentrations of P solutions in 0.01

109   mol L^{-1} NaCl background. The solution pH was adjusted to 8.5 ± 0.05 with 0.10 mol

110   L^{-1} HCl and 0.10 mol L^{-1} NaOH and shaken at 170 rpm at 25 °C for 48 h. Zeta (ζ)

111   potentials of LAH samples after P adsorption were measured by a Zetasizer Nano ZS

112   potential analyzer (Malvern, United Kingdom). The P adsorption capacities of LAH

113   and Phoslock were also determined with initial P concentration 1 mmol L^{-1} at pH 8.5

114   ± 0.05 under 0.01 mol L^{-1} NaCl background.

115   In order to explore P desorption capacity of LAH, the desorption experiments were

116   conducted. Adsorbents (1 g L^{-1}) were added to 50 mL polypropylene tubes with initial

117   P concentration 1 mmol L^{-1} in 0.01 mol L^{-1} NaCl background. The solution pH was

118   adjusted to 8.5 ± 0.05 and shaken at 25 °C for 48 h. After the adsorption equilibrium

119   was reached, the exhausted solutions were centrifuged to preserve 10 mL suspension

120   at the bottom, and 0.01 mol L^{-1} NaCl solution was added to keep the same ionic

121   strength. The experimental conditions of desorption experiments were carried out the

122   same as former adsorption studies.

The concentrations of Ortho-P were measured by ascorbic acid method using a UV-756 PC spectrophotometer at 880 nm (Shanghai Sunny Hengping Scientific Instrument CO. Ltd., China). IHP and Pyro-P were hydrolyzed to inorganic phosphate by persulfate acid digestion and then determined using the same method as Ortho-P.[27, 28]

2.4. Adsorption kinetic experiments.

The adsorption kinetic experiments were carried out with initial P concentration 1 mmol L^{-1} in 0.01 mol L^{-1} NaCl background. The solution pH was maintained at 8.5 ± 0.05 and the contact time was from 0 h to 48 h. The samples were taken over a period of time and filtered through a 0.45 µm syringe nylon-membrane filter. The P concentration was determined as the former method in adsorption and desorption experiments.

2.5. Solid-state ^{31}P nuclear magnetic resonance measurements.

Solid-state ^{31}P nuclear magnetic resonance (NMR) spectra of LAH adsorption samples were obtained on a 600 MHz JNM-ECZ600R/M1 spectrometer (14.1 T) at ambient temperature (22 °C). The ^{31}P operating frequency was 242.95 MHz. Samples were contained in 3.2 mm (o.d.) ZrO_2 rotors at a spinning rate of 10 kHz. The ^{31}P spectra were obtained with an excitation 40° pulse of 0.1 µs with a 2 s relaxation delay. The pulse delay was optimized at 2 s to obtain an optimal signal-to-noise ratio.

2.6. P K-edge XANES data collection and analysis.

All XANES spectra were obtained in fluorescence yield mode at Beamline 4B7A at the Beijing Synchrotron Radiation Facility (BSRF), China. Measurements were conducted at energy ranging from −30 to +90 eV relative to P K-edge energy at 2152 eV with a minimum step size of 0.2 eV between 2140 and 2180 eV. Each spectrum was baseline corrected and normalized by ATHENA program.[29] The proportions of

148 Ortho-P, IHP, and Pyro-P bonded on La- and Al- hydroxides in LAH samples were

149 determined by liner combination fitting (LCF) analysis. Samples of three P

150 compounds bonded on contrast adsorbents La(OH)$_3$ and Al(OH)$_3$ with Ortho-P (30.9

151 mg P g^{-1} La/15.7 mg P g^{-1} Al), IHP (30.8 mg P g^{-1} La/18.7 mg P g^{-1} Al) and Pyro-P

152 (13.0 mg P g^{-1} La/14.7 mg P g^{-1} Al) were used as standards in LCF analysis,

153 respectively.

154 **3. RESULTS**

155 **3.1. Phosphate adsorption and desorption.**

156 The IHP and Pyro-P adsorption isotherms for LAH were L-curves (Figure 1) and

157 were fitted to Langmuir equation with r^2 values of 0.999 and 0.999, respectively

158 (Table S1). The maximum IHP and Pyro-P adsorption capacities by LAH were 36.4

159 mg P g^{-1} and 21.8 mg P g^{-1}, respectively. The ratio of Q$_m$ (Ortho-P)/Q$_m$ (IHP) was 1.9,

160 suggesting that IHP may bind on LAH surface through two of its six phosphate groups

161 and with the other four phosphate groups free and dissociated. Compared to

162 commercial product Phoslock, the Ortho-P, IHP, and Pyro-P adsorption capacities of

163 LAH were 2.7, 1.1, and 3.0 times higher than those of Phoslock at initial P

164 concentration 1 mmol L^{-1} at pH 8.5, respectively (Figure S1).
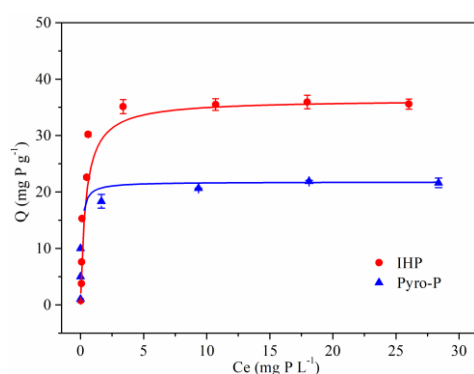

165

166 **Figure 1.** Langmuir adsorption isotherms of IHP and Pyro-P on LAH. The

8

167   experimental condition: temperature =25°C, adsorbent dosage =1 g L^{-1}, pH =8.5, and

168   reaction time =48 h.

169   The ζ potentials of LAH samples after P adsorption all showed a decreasing trend

170   with increasing P adsorption amounts (Figure 2). Additionally, LAH samples with IHP

171   bonded had relatively lower ζ potentials than those of Ortho-P (Figure 2). The P

172   desorption on LAH was also conducted at initial P concentration 1 mmol L^{-1} at pH 8.5

173   (Figure S2). The results showed that the desorption rates of Ortho-P, IHP, and Pyro-P

174   of LAH were 0.16%, 0.28%, and 0.40% (Figure S2), respectively.
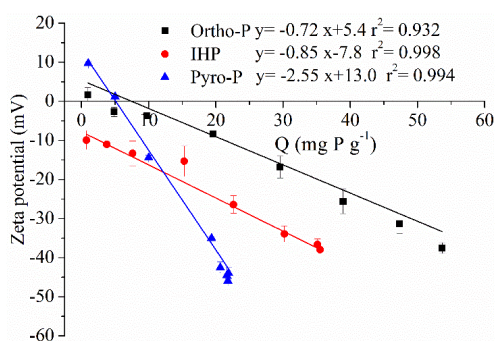
175

176   **Figure 2.** The ζ potentials of LAH after Ortho-P, IHP, and Pyro-P adsorption as a

177   function of total P bonded amounts. Regression fits to the data are shown as solid

178   lines.

179   **3.2. Phosphate adsorption kinetics.**

180   The adsorption kinetic studies of LAH with Ortho-P, IHP, and Pyro-P were shown in

181   Figure 3. The P adsorption capacities of LAH all increased with contacting time and

182   then kept equilibrium. Ortho-P, IHP, and Pyro-P bonded on LAH reached equilibrium

183   after 24 h, 20 h, and 24 h at initial P concentration 1 mmol L^{-1} (Figure 3a),

184   respectively. The adsorption of Ortho-P, IHP, and Pyro-P followed the pseudo-second

185   order kinetics with r^2 values of 0.999, 0.999, and 0.997 (Table S2), respectively. The

186   rate constants (K) of LAH with Ortho-P, IHP, and Pyro-P were 0.052, 0.064, and

187   0.052 g mg^{-1} h^{-1}, respectively.
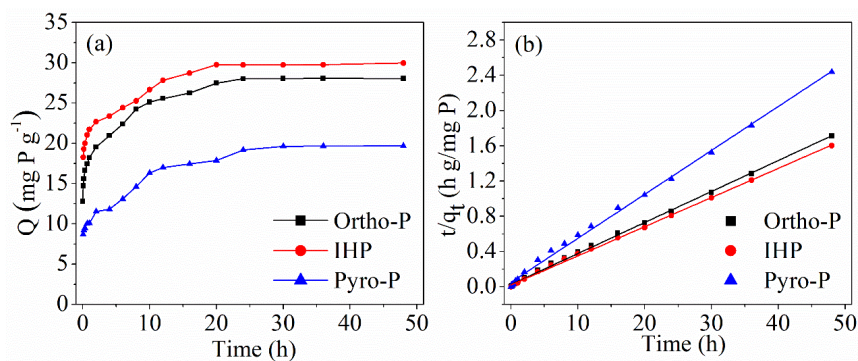
188

189 **Figure 3.** Kinetic studies for Ortho-P, IHP, and Pyro-P adsorption on LAH (a) and its

190 pseudo-second-order fitting plots (b). The experimental condition: temperature =25°C,

191 adsorbent dosage =1 g L^{-1}, pH =8.5, and reaction time =48 h.

192 **3.3. Solid-state ^{31}P NMR.**

193   The ^{31}P SSNMR spectra for P bonded on LAH were shown in Figure 4. The ^{31}P

194 NMR spectrum of Ortho-P bonded on LAH had two major resonances with chemical

195 shifts at δ_{P-31} = 2.00 and -1.95 ppm. The ^{31}P NMR spectrum of IHP bonded on LAH

196 exhibited a main peak at δ_{P-31} = -0.76 ppm with a shoulder at δ_{P-31} = -3.47 ppm. The

197 spectrum for Pyro-P bonded on LAH showed two major peaks at δ_{P-31} = -4.33 and
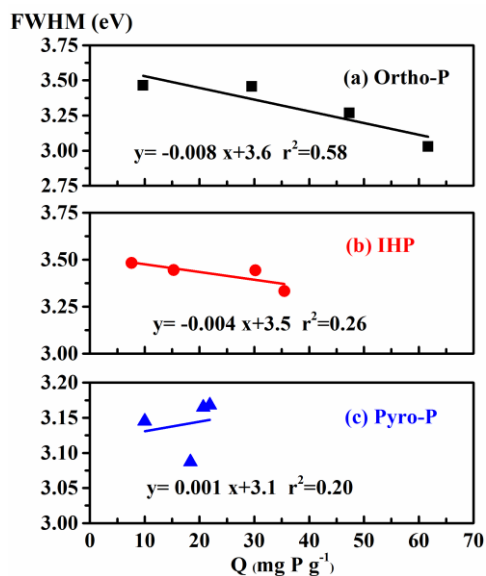
198 -5.74 ppm.

199
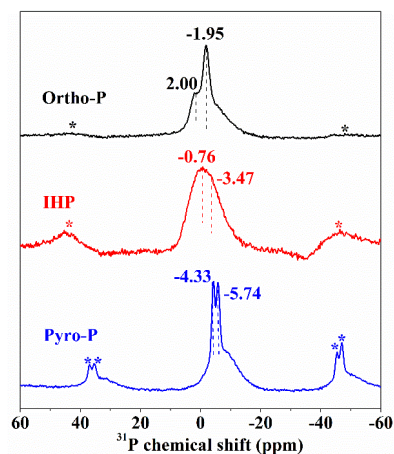
Figure 4. Solid-state ^{31}P NMR spectra of Ortho-P, IHP, and Pyro-P bonded on LAH

with initial P concentration 2 mmol L^{-1} at pH 8.5.

3.4. P K-edge XANES.

  Normalized P K-edge XANES spectra for Ortho-P, IHP, and Pyro-P bonded on LAH

were shown in Figure S3. The full width at half-maximum height (fwhm) of

white-line peaks of XANES spectra for P bonded on LAH as a function of P adsorbed

amounts were shown in Figure 5. The trends indicated that there were no positive

correlations between the fwhm and Ortho-P, IHP, and Pyro-P due to the low r^2 values

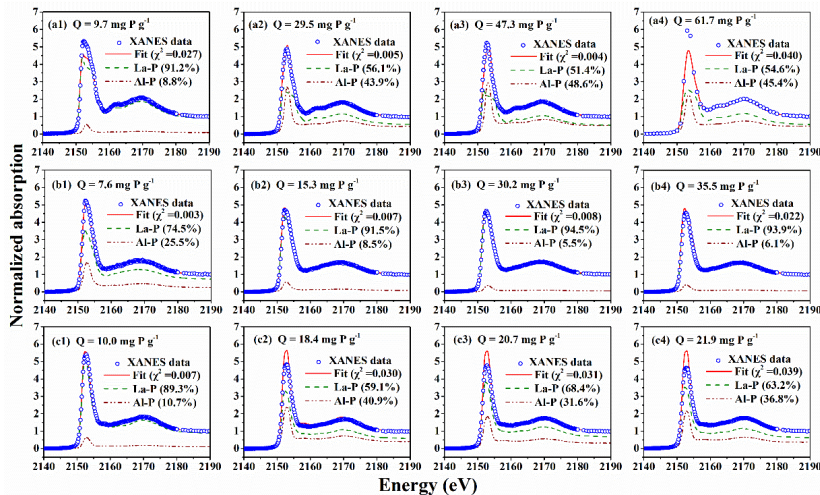(0.58, 0.26, and 0.20, respectively) for linear regressions.

11

FWHM (eV)

(a) Ortho-P

$y = -0.008\ x + 3.6\quad r^2 = 0.58$

(b) IHP

$y = -0.004\ x + 3.5\quad r^2 = 0.26$

(c) Pyro-P

$y = 0.001\ x + 3.1\quad r^2 = 0.20$

$Q\ (mg\ P\ g^{-1})$

Figure 5. The fwhm of the white-line peaks of XANES spectra for Ortho-P (a), IHP (b), and Pyro-P (c) bonded on LAH as a function of P adsorbed amounts. Regression fits to the data are shown as solid lines.

According to our previous study, LAH were mainly composed of $Al(OH)_3$ and $La(OH)_3$.[10] The distribution proportions of Ortho-P, IHP, and Pyro-P bonded on La-hydroxide and Al-hydroxide were determined using LCF analysis.[30, 31] LCF results showed that the proportions of Ortho-P bonded with La-hydroxide (La-P) were 51.4% - 91.2%, which were higher than those with Al-hydroxide (Al-P) of 48.6% - 8.8% (Figure 6 a1-a4). For LAH samples with IHP bonded, the proportions of IHP associated with La-hydroxide (La-P, 74.5% - 94.5%) were much higher than those with Al-hydroxide (Al-P, 25.5% - 5.5%) (Figure 6 b1-b4). Additionally, the proportions of Pyro-P bonded with La-hydroxide (La-P, 59.1% - 89.3%) in LAH were also higher than those with Al-hydroxide (Al-P, 40.9% - 10.7%) (Figure 6 c1-c4).

Figure 6. Linear combination fitting for LAH samples after Ortho-P (a), IHP (b), and Pyro-P (c) adsorption with weighted components of La-P and Al-P.

4. DISCUSSION

4.1. Phosphate adsorption on LAH

Compared to the positive ζ potential of pristine LAH (+10 mV) at pH 8.5,[10] the ζ potentials of LAH samples with Ortho-P, IHP, and Pyro-P bonded all decreased with increasing P adsorbed amounts (Figure 2). The results might suggest that three P species were bonded on LAH surfaces by forming inner sphere complexes.[32, 33] The ζ potentials of LAH samples with Ortho-P, IHP, and Pyro-P bonded were linearly related to the total P adsorbed amounts with r^2 values of 0.932, 0.998, and 0.994 (Figure 2), respectively. Such trends of ζ potentials indicated that the process of surface adsorption occurred in the reaction between LAH and three P species.[34] Because if surface precipitation dominated in the interaction process, there would be no significant change in the surface groups responsible for surface charge i.e. ζ potentials.[34] Additionally, the adsorption kinetics of Ortho-P, IHP, and Pyro-P were all fitted to the pseudo-second-order model (Table S2), possibly suggesting that the

13

240 process of P adsorption on LAH might be chemisorption.[35] For the ^{31}P SSNMR

241 spectra, it was reported that the chemical shifts of nonreacted Ortho-P, IHP, and

242 Pyro-P appeared at δ_{P-31} = 1.31, -0.5, and -4.65 ppm, respectively.[24, 36] In this study,

243 the peaks in the ^{31}P SSNMR spectra of Ortho-P, IHP, and Pyro-P bonded on LAH at

244 δ_{P-31} = 2.00, -0.76, and -4.33 ppm could thus be assigned to the free phosphate groups

245 adsorbed on LAH. While the peaks at δ_{P-31} = -1.95, -3.47, and -5.74 ppm could be

246 attributed to the phosphate groups bonded on LAH (Figure 4), respectively.[19, 37, 38]

247 Some studies have demonstrated that surface precipitates was shifted to high negative

248 field (δ_{P-31} = -11 to -30 ppm) and signals appearing between 0 and -11 ppm were due

249 to inner-sphere complexes.[37] Hence, the results of ^{31}P NMR analysis further indicated

250 that the formation of inner-sphere P surface complexes was the dominant mechanism

251 on LAH surfaces.

252   In order to illustrate the mechanism of surface adsorption at the molecular level, we

253 have determined the P K-edge XANES spectra (Figure S3) and calculated the fwhm

254 of white-line peaks of XANES spectra for samples of Ortho-P, IHP, and Pyro-P

255 bonded on LAH (Figure 5). The fwhm values of spectra for Ortho-P, IHP, and Pyro-P

256 bonded on LAH showed no positive correlations with the total P sorbed amounts

257 (Figure 5), respectively. It was reported that surface precipitate of Al-phosphate was

258 formed on the basis of the evidence that the fwhm of the white-line peaks in XANES

259 spectra for Ortho-P bonded on boehmite, non-xl Al-hydroxide or goethite-boehmite

260 mixtures positively correlated with increasing total Ortho-P sorbed amounts.[31] The

261 XANES information possibly provided strong evidence that it is surface adsorption

262 not precipitation played a role in the adsorption of Ortho-P, IHP, and Pyro-P by LAH.

263 In our previous study, we have found that there were oxygen defects on LAH surfaces,

264 which might provide special adsorption sites to Ortho-P.[10] Hence, we could infer that

265   these oxygen defects might also present as active adsorption sites for IHP and Pyro-P.

266   Adsorption isotherm results showed that IHP could bond on LAH surfaces through

267   two of its six phosphate groups (Table S1), thus resulting in more negative surface

268   charge of LAH with adsorbed IHP than those of Ortho-P (Figure 2). Owing to the

269   much stronger negative surface charge of IHP,[39] it could be removed a little faster (20

270   h, Figure 3) via stronger electrostatic attraction compared to Ortho-P and Pyro-P (24 h,

271   Figure 3). However, because IHP had a larger molecule size and stronger steric

272   hindrance than Ortho-P,[40, 41] the maximum IHP binding capacity of LAH (36.4 mg P

273   g^{-1}, Table S1) was less than that of Ortho-P (70.4 mg P g^{-1}).[8] Moreover, LAH had the

274   lowest adsorption capacity of Pyro-P (21.8 mg P g^{-1}, Table S1), which possibly

275   because that Pyro-P had a weaker metal-complexing power owing to its cyclic

276   structure.[42]

277   **4.2. P distribution on LAH**

278   The distribution proportions of Ortho-P, IHP, and Pyro-P bonded on La-hydroxide

279   and Al-hydroxide in LAH were obtained by LCF analysis.[25, 43] The proportion of

280   Ortho-P associated with La-hydroxide were 10.4 times higher than that with

281   Al-hydroxide when total Ortho-P adsorbed amount was 9.7 mg P g^{-1} at pH 8.5 (Figure

282   6a1). With increasing Ortho-P adsorbed amounts (29.5, 47.3, and 61.7 mg P g^{-1},

283   respectively), the proportions of Ortho-P bonded with La-hydroxide were 1.3, 1.1, and

284   1.2 times higher than those with Al-hydroxide (Figure 6a2-a4). The fitting data about

285   Ortho-P indicated that the adsorption active sites on La-hydroxide might tend to

286   become saturated compared to lower Ortho-P adsorbed amount (9.7 mg P g^{-1}). For

287   IHP, it was reported that IHP was initially adsorbed on amorphous Al-hydroxide and

288   then transformed to surface precipitates from pH 3.5 to pH 7.0.[24] In this study,

289   according to P K-edge XANES and ^{31}P SSNMR analyses, our work demonstrated that

290   IHP always showed a more preferable distributions on La-hydroxide (74.5% - 94.5%,

291   Figure 6b) than those with Al-hydroxide (25.5% - 5.5%, Figure 6b) in LAH via

292   surface adsorption at alkaline condition pH 8.5. Additionally, Pyro-P was

293   preferentially bonded with La-hydroxide at pH 8.5 depending on the higher Pyro-P

294   proportions associated with La-hydroxide (59.1% - 89.3%, Figure 6c) than those of

295   Al-hydroxide (40.9% - 10.7%, Figure 6c). The LCF analysis showed that

296   La-hydroxide had a remarkable P binding ability to different P species at the

297   molecular level. The preferences of Ortho-P, IHP, and Pyro-P on La-hydroxide and

298   Al-hydroxide might provide a theoretical guidance to synthesize novel P locking

299   materials for various P species removal in water treatment.

300   **4.3. Environmental implications**

301   The interfacial reactions between different P species (e.g. inorganic phosphate,

302   organic phosphate, and condensed phosphate) and lake restoration materials can

303   greatly influence the transformation, mobility, and dynamics of P and the chemistry of

304   materials in natural systems, thus affecting the biomass production of ecosystems.[44]

305   Our study is the first to determine the adsorption properties and interaction

306   mechanisms of different P species such as Ortho-P, IHP, and Pyro-P on

307   La/Al-hydroxide composite. It advances the knowledge of using La-bearing materials

308   for effective adsorption of different P species. Our previous studies have demonstrated

309   that LAH had the highest Ortho-P adsorption capacity at pH 4.0 and relatively lower

310   Ortho-P adsorption capacity at pH 8.5.[10] In this study, all the experiments were

311   conducted at pH 8.5. The results showed that LAH also has excellent adsorption

312   capacities to IHP and Pyro-P compared to commercial available Phoslock (Figure S1),

313   which could significantly control the concentration of total P in water bodies and

314   block excessive P source for aquatic organisms growing. Owing to higher P binding

315 ability to La-hydroxide (Figure 6), LAH exhibited low P desorption rates at typical

316 lake pH 8.5 (Figure S2). Our work has demonstrated that P was bonded on LAH

317 surface via adsorption mechanism not surface precipitation, which might be a stable P

318 storage from the view of P recycling. To better understand the environmental behavior

319 of LAH when using in geo-engineering lake restoration, further studies with respect to

320 the interaction between LAH and different P species dissolved from sediments should

321 be taken into account.[45] According to LCF analysis, we can exactly determine the

322 contribution of La-hydroxide versus Al-hydroxide to different P species in LAH. Such

323 molecular level information could also provide a guide to develop new

324 multifunctional P removal materials in the future.

325 **5. Conclusions**

326   In this study, the removal efficiencies and adsorption mechanisms of IHP and

327 Pyro-P with the contrast of Ortho-P by LAH composite were investigated. The

328 maximum IHP and Pyro-P adsorption capacities by LAH were 36.4 mg P g^{-1} and 21.8

329 mg P g^{-1}, respectively. The ζ potentials of LAH samples with Ortho-P, IHP, and

330 Pyro-P bonded all decreased with increasing P adsorbed amounts. For the ^{31}P SSNMR

331 spectra, the peaks at δ_{P-31} = -1.95, -3.47, and -5.74 ppm could be attributed to the

332 phosphate groups bonded on LAH, respectively. The trends of fwhm indicated that

333 there were no positive correlations between the fwhm and Ortho-P, IHP, and Pyro-P

334 due to the low r^2 values (0.58, 0.26, and 0.20, respectively) for linear regressions. The

335 LCF analysis showed that La-hydroxide had a remarkable P binding ability to

336 different P species at the molecular level. Zeta potential, NMR spectroscopy and P

337 K-edge XANES analyses possibly indicated that the interaction between LAH and P

338 species was surface adsorption by the formation of inner-sphere complexes.

339 **ASSOCIATED CONTENT**

Supporting Information

More detailed information about (1) Langmuir isotherm parameters of LAH (Table S1); (2) pseudo-second-order model constants and correlation coefficients of LAH (Table S2); (3) P adsorption capacities of LAH and Phoslock (Figure S1); (4) P desorption rates to LAH (Figure S2); and (5) normalized XANES spectra of LAH with bonded Ortho-P, IHP, and Pyro-P (Figure S3).

AUTHOR INFORMATION

Corresponding Authors

*E-mail: myzhang@rcees.ac.cn.

*E-mail: gpan@rcees.ac.cn. Tel.: +86 10 62849686; Fax: +86 10 62849686.

Notes

The authors declare no competing financial interest.

REFERENCES

1. Conley, D. J.; Paerl, H. W.; Howarth, R. W.; Boesch, D. F.; Seitzinger, S. P.; Havens, K. E.; Lancelot, C.; Likens, G. E., Controlling eutrophication: nitrogen and phosphorus. *Science* **2009,** *323*, (20), 1014-1015.

2. Smith, V. H.; Tilman, G. D.; Nekola, J. C., Eutrophication: impacts of excess nutrient inputs on freshwater, marine, and terrestrial ecosystems. *Environ. Pollut.*

18

364   **1999,** *100*, 179-196.

365   3.   Douglas, G. B.; Hamilton, D. P.; Robb, M. S.; Pan, G.; Spears, B. M.; Lürling, M.,

366   Guiding principles for the development and application of solid-phase phosphorus

367   adsorbents for freshwater ecosystems. *Aquat. Ecol.* **2016**, 1-21.

368   4.   Shin, E. W.; Karthikeyan, K. G.; Tshabalala, M. A., Orthophosphate sorption onto

369   lanthanum treated lignocellulosic sorbents. *Environ. Sci. Technol.* **2005,** *39*, (16),

370   6273-6279.

371   5.   Yang, J.; Yuan, P.; Chen, H.-Y.; Zou, J.; Yuan, Z. G.; Yu, C. Z., Rationally

372   designed functional macroporous materials as new adsorbents for efficient phosphorus

373   removal. *J. Mater. Chem.* **2012,** *22*, (19), 9983-9990.

374   6.   Yu, J.; Xiang, C.; Zhang, G.; Wang, H.; Ji, Q.; Qu, J., Activation of lattice oxygen

375   in LaFe (Oxy)hydroxides for efficient phosphorus removal. *Environ. Sci. Technol.*

376   **2019,** *53*, (15), 9073-9080.

377   7.   Fang, L.; Liu, R.; Li, J.; Xu, C.; Huang, L. Z.; Wang, D., Magnetite/Lanthanum

378   hydroxide for phosphate sequestration and recovery from lake and the attenuation

379   effects of sediment particles. *Water Res.* **2018,** *130*, 243-254.

380   8.   Smith, V. H., *Cultural eutrophication of inland, estuarine, and coastal waters*.

381   Springer: New York, 1998; p 7-49.

382   9.   Ahlgren, J.; Reitzel, K.; Danielsson, R.; Gogoll, A.; Rydin, E., Biogenic

383   phosphorus in oligotrophic mountain lake sediments: differences in composition

384   measured with NMR spectroscopy. *Water Res.* **2006,** *40*, (20), 3705-3712.

385   10. Xu R.; Zhang M. Y.; Robert J.G. Mortimer; Pan, G., Enhanced phosphorus

locking by novel lanthanum/aluminum− hydroxide composite: Implications for eutrophication control. *Environ. Sci. Technol.* **2017,** *51*, (6), 3418-3425.

11. Correll, D. L., The role of phosphorus in the eutrophication of receiving waters: A review. *J. Environ. Qual* **1998,** *27*, (2), 261-266.

12. Groot, C. J. D.; Golterman, H. L., On the presence of organic phosphate in some Camargue sediments: evidence for the importance of phytate. *Hydrobiologia* **1993,** *252*, (1), 117-126.

13. Turner, B. L.; Cheesman, A. W.; Godage, H. Y.; Riley, A. M.; Potter, B. V., Determination of neo- and D-chiro-inositol hexakisphosphate in soils by solution ^{31}P NMR spectroscopy. *Environ. Sci. Technol.* **2012,** *46*, (9), 4994-5002.

14. Suzumura M.; A., K., Mineralization of inositol hexaphosphate in aerobic and anaerobic marine sediments: Implications for the phosphorus cycle. *Geochimica et Cosmochimica Acta* **1995,** *59*, (5), 1021-1026.

15. R.P. Dick; Tabatabai, M. A., Polyphosphates as sources of phosphorus for plants. *Fertilizer Research* **1987,** *12*, (2), 107-118.

16. Ignacio Hernandez; Abraham P ́erez-Pastor; ́ens, J. L. P. e. L., Ecological significance of phosphomonoesters and phosphomonoesterase activity in a small Mediterranean river and its estuary. *Aquatic Ecology* **2000,** *34*, (2), 107-117.

17. Dyhrman, S. T.; Chappell, P. D.; Haley, S. T.; Moffett, J. W.; Orchard, E. D.; Waterbury, J. B.; Webb, E. A., Phosphonate utilization by the globally important marine diazotroph Trichodesmium. *Nature* **2006,** *439*, (7072), 68-71.

18. Sundareshwar;, P. V.; Morris;, J. T.; Pellechia;, P. J.; Cohen;, H. J.; Porter;, D. E.;

408   Jones, B. C., Occurrence and ecological implications of pyrophosphate in estuaries.

409   *Limnol. Oceanogr.* **2001,** *46*, (6), 1570-1577.

410   19. Wan, B.; Yan, Y. P.; Liu, F.; Tan, W. F.; He, J. J.; Feng, X. H., Surface speciation

411   of *myo*-inositol hexakisphosphate adsorbed on TiO_2 nanoparticles and its impact on

412   their colloidal stability in aqueous suspension: A comparative study with

413   orthophosphate. *Sci. Total. Environ.* **2016,** *544*, 134-142.

414   20. Yan, Y.; Koopal, L. K.; Li, W.; Zheng, A.; Yang, J.; Liu, F.; Feng, X.,

415   Size-dependent sorption of myo-inositol hexakisphosphate and orthophosphate on

416   nano-gamma-Al2O3. *Journal of colloid and interface science* **2015,** *451*, 85-92.

417   21. Guan, X. H.; Liu, Q.; Chen, G. H.; Shang, C., Surface complexation of condensed

418   phosphate to aluminum hydroxide: an ATR-FTIR spectroscopic investigation. *Journal*

419   *of colloid and interface science* **2005,** *289*, (2), 319-27.

420   22. Kim, J.; Li, W.; Philips, B. L.; Grey, C. P., Phosphate adsorption on the iron

421   oxyhydroxides goethite (α-FeOOH), akaganeite (β-FeOOH), and lepidocrocite

422   (γ-FeOOH): a 31P NMR Study. *Energy & Environmental Science* **2011,** *4*, (10),

423   4298-4305.

424   23. Van Emmerik, T. J.; Sandström, D. E.; Antzutkin, O. N.; Angove, M. J.; Johnson,

425   B. B., ^{31}P solid-state nuclear magnetic resonance study of the sorption of phosphate

426   onto gibbsite and kaolinite. *Langmuir* **2007,** *23*, (6), 3205-3213.

427   24. Yan, Y.; Li, W.; Yang, J.; Zheng, A.; Liu, F.; Feng, X.; Sparks, D. L., Mechanism

428   of myo-inositol hexakisphosphate sorption on amorphous aluminum hydroxide:

429   spectroscopic evidence for rapid surface precipitation. *Environmental science &*

430   *technology* **2014,** *48*, (12), 6735-42.

431   25. Liu, J.; Hu, Y. F.; Yang, J. J.; Abdi, D.; Cade-Menun, B. J., Investigation of soil

432   legacy phosphorus transformation in long-term agricultural fields using sequential

433   fractionation, P K-edge XANES and solution P NMR spectroscopy. *Environ. Sci.*

434   *Technol.* **2015,** *49*, (1), 168-176.

435   26. Werner, F.; Prietzel, J., Standard Protocol and Quality Assessment of Soil

436   Phosphorus Speciation by P K-Edge XANES Spectroscopy. *Environmental science &*

437   *technology* **2015,** *49*, (17), 10521-8.

438   27. Martin, M.; Celi, L.; Barberis, E., Determination of low concentrations of organic

439   phosphorus in soil solution. *Commun. Soil Sci. and Plan.* **1999,** *30*, (13-14),

440   1909-1917.

441   28. Georgantas, D. A.; Grigoropoulou, H. P., Orthophosphate and metaphosphate ion

442   removal from aqueous solution using alum and aluminum hydroxide. *Journal of*

443   *colloid and interface science* **2007,** *315*, (1), 70-9.

444   29. Ravel, B.; Newville, M., ATHENA, ARTEMIS, HEPHAESTUS: data analysis for

445   X-ray absorption spectroscopy using IFEFFIT. *J. Synchrotron Radiat.* **2005,** *12*, (Pt 4),

446   537-541.

447   30. Liu, Y. T.; Hesterberg, D., Phosphate bonding on noncrystalline Al/Fe-hydroxide

448   coprecipitates. *Environ. Sci. Technol.* **2011,** *45*, (15), 6283-6289.

449   31. Khare, N.; Hesterberg, D.; Martin, J. D., XANES investigation of phosphate

450   sorption in single and binary systems of iron and aluminum oxide minerals. *Environ.*

451   *Sci. Technol.* **2005,** *39*, (7), 2152-2160.

452 32. Wan, B.; Yan, Y. P.; Liu, F.; Tan, W. F.; He, J. J.; Feng, X. H., Surface speciation

453 of myo-inositol hexakisphosphate adsorbed on TiO_2 nanoparticles and its impact on

454 their colloidal stability in aqueous suspension: A comparative study with

455 orthophosphate. *Sci. Total Environ.* **2016,** *544*, 134-142.

456 33. Antelo, J.; Avena, M.; Fiol, S.; Lopez, R.; Arce, F., Effects of pH and ionic

457 strength on the adsorption of phosphate and arsenate at the goethite-water interface. *J.*

458 *Colloid Interface Sci.* **2005,** *285*, (2), 476-486.

459 34. Li, L.; Stanforth, R., Distinguishing adsorption and surface precipitation of

460 phosphate on goethite (alpha-FeOOH). *J. Colloid Interface Sci.* **2000,** *230*, (1), 12-21.

461 35. Huang, W. Y.; Li, D.; Liu, Z. Q.; Tao, Q.; Zhu, Y.; Yang, J.; Zhang, Y. M.,

462 Kinetics, isotherm, thermodynamic, and adsorption mechanism studies of

463 La(OH)$_3$-modified exfoliated vermiculites as highly efficient phosphate adsorbents.

464 *Chem. Eng. J.* **2014,** *236*, (2), 191-201.

465 36. Ye Ru han; Chen Yong; Liu Ya Ling; Zhu Li Ming; Li Zheng Quan; Sun Yi Feng;

466 Long, P. W., Analysis of phosphorus-containing compounds in detergents by [31]P

467 nuclear magnetic resonance. *Journal of Instrumental Analysis* **2011,** *30*, (6), 624-628.

468 37. Li, W.; Pierre-Louis, A.-M.; Kwon, K. D.; Kubicki, J. D.; Strongin, D. R.; Phillips,

469 B. L., Molecular level investigations of phosphate sorption on corundum (α-Al_2O_3) by

470 ^{31}P solid state NMR, ATR-FTIR and quantum chemical calculation. *Geochim.*

471 *Cosmochim. Ac.* **2013,** *107*, 252-266.

472 38. Sannigrahi, P., Polyphosphates as a source of enhanced P fluxes in marine

473 sediments overlain by anoxic waters: Evidence from ^{31}P NMR. *Geochem. Trans.* **2005,**

474 *6*, (3), 52-59.

475 39. Wan, B.; Yan, Y. P.; Liu, F.; Tan, W. F.; He, J. J.; Feng, X. H., Effects of

476 myo-inositol hexakisphosphate and orthophosphate adsorption on aggregation of

477 CeO$_2$ nanoparticles: roles of pH and surface coverage. *Environmental Chemistry* **2016,**

478 *13*, (1), 34-42.

479 40. Ruttenberg, K. C.; Sulak, D. J., Sorption and desorption of dissolved organic

480 phosphorus onto iron (oxyhydr)oxides in seawater. *Geochimica et Cosmochimica*

481 *Acta* **2011,** *75*, (15), 4095-4112.

482 41. Yan, Y. P.; Koopal, L. K.; Li, W.; Zheng, A. M.; Yang, J.; Liu, F.; Feng, X. H.,

483 Size-dependent sorption of myo-inositol hexakisphosphate and orthophosphate on

484 nano-gamma-Al$_2$O$_3$. *J. Colloid Interface Sci.* **2015,** *451*, 85-92.

485 42. Corbridge, D. E., *Phosphorus: an outline of its chemistry, biochemistry and uses*.

486 Elsevier Science: Netherlands, 1992.

487 43. Andersson, K. O.; Tighe, M. K.; Guppy, C. N.; Milham, P. J.; McLaren, T. I.;

488 Schefe, C. R.; Lombi, E., XANES demonstrates the release of calcium phosphates

489 from alkaline vertisols to moderately acidified solution. *Environ. Sci. Technol.* **2016,**

490 *50*, (8), 4229-4237.

491 44. de Vicente, I.; Jensen, H. S.; Andersen, F. O., Factors affecting phosphate

492 adsorption to aluminum in lake water: implications for lake restoration. *Sci. Total*

493 *Environ.* **2008,** *389*, (1), 29-36.

494 45. Huang, X. L.; Zhang, J. Z., Spatial variation in sediment-water exchange of

495 phosphorus in florida bay: AMP as a model organic compound. *Environ. Sci. Technol.*

496   **2010,** *44*, (20), 7790-7795.